Available online at www.sciencedirect.com
SCIENCE DIRECT®
Surface Science 584 (2005) 214–224
SURFACE SCIENCE
www.elsevier.com/locate/susc

NO restructuring of surface Ir and bond formation to preadsorbed O on Ir{100} at 95 K

Sabyasachi Khatua, Zhi-Pan Liu, David A. King *

Department of Chemistry, University of Cambridge, Lensfield Road, Cambridge CB2 1EW, United Kingdom

Received 14 February 2005; accepted for publication 5 April 2005
Available online 18 April 2005

Abstract

RAIRS experiments and density functional theory calculations have been performed to understand the adsorption behavior of nitric oxide on different phases of Ir{100} at 95 K, namely, Ir{100}-(1 × 1), Ir{100}-(1 × 5), and O-precovered Ir{100}-(1 × 1) surfaces. Molecular NO adsorption is observed on all the phases and the adsorption structures of NO on the surfaces are determined. Mixed isotope experiments verify that no $(NO)_2$ dimer is formed on the surfaces. Importantly, at an NO coverage of ~0.3 ML, a local lifting of reconstruction from the (1 × 5) to the (1 × 1) phase occurs, which is found to be driven by the preferential adsorption of NO on the (1 × 1) phase. On the O-precovered Ir{100} surface, an unusual $NO^{\delta+}$ species is identified, featuring a stretching frequency 30–60 cm^{-1} higher than the NO gas phase frequency. This $NO^{\delta+}$ species is suggested to be NO bonded to preadsorbed O atoms rather than surface Ir atoms.

Keywords: Nitric oxide; Iridium surfaces; Surface infrared spectroscopy; Density functional theory

1. Introduction

The interaction of NO with Ir has attracted much recent attention since Ir was found to be one of the most promising metals to reduce NO to N_2 under oxidative conditions, a key process towards reducing pollution caused by vehicle exhausts [1–5]. Among the low-index surfaces that are mostly available in Ir particle catalysts, the Ir{100} surface deserves more attention than it has been given. An important property of Ir{100} is that the clean Ir{100}-(1 × 1) phase (bulk-truncated phase) will reconstruct to a stable (1 × 5) phase (a {111}-like surface) at elevated temperatures (see Fig. 1). The reconstruction can be lifted by adsorbates (e.g. CO and NO). Because the (1 × 5) surface is 20% denser than the (1 × 1)

* Corresponding author. Tel.: +44 1223336502; fax: +44 1223336536.
E-mail addresses: zl222@cam.ac.uk (Z.-P. Liu), dak10@cam.ac.uk (D.A. King).

0039-6028/$ - see front matter © 2005 Published by Elsevier B.V.
doi:10.1016/j.susc.2005.04.002

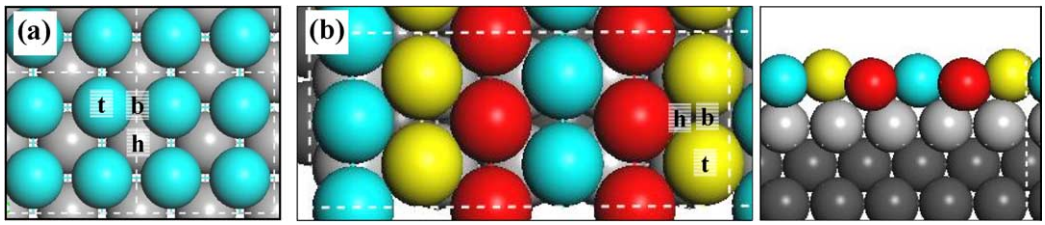

Fig. 1. Ir{100}-(1 × 1) (a) and Ir{100}-(1 × 5) (b: top and side view). The structure in the figure is obtained from DFT calculations and LEED structural analysis [23]. The labels t, b and h in the figure represent the top site, the bridge site and the hollow site, respectively.

surface, a change in reactivity is certainly expected on going from one phase to another. This is a phenomenon generally known as structure sensitivity in heterogeneous catalysis. Towards the design of better catalysts for NO reduction on Ir-based catalysts, a molecular-level understanding of NO interaction with Ir{100} is essential. Combining RAIRS experiment and density functional theory (DFT) calculations, here we report a detailed study of NO adsorption on three different phases of Ir{100} at 95 K, namely, Ir{100}-(1 × 5), Ir{100}-(1 × 1) and O-precovered Ir{100}-(1 × 1) surfaces.

Experimentally, a typical approach to study NO adsorption on metal surfaces is to measure the NO stretching frequency as a function of increasing coverage [6]. It is, however, not always straightforward to assign the adsorption sites for NO on metal surfaces. Recently it was realized that assignments of NO IR bands on metal surfaces based on the frequencies of organometallic metal nitrosyls can be misleading [6]. There are two major reasons. First, the electronic structure of NO on metal surfaces is quite different from its organometallic counterpart because of the interference of metal delocalized electrons at the Fermi level. Secondly, on metal surfaces band intensity transfer often occurs with increase in coverage, attributable to the dynamic dipole–dipole coupling [7]. For instance, Severson et al. [8] have performed some model calculations of the densely packed (2 × 2)-3CO structure on the Pt{111} surface and observed that a considerable amount of intensity is transferred from the three-fold hollow site (low frequency) to the atop site (high frequency) whose singleton frequencies are substantially different, by $\sim$280 cm^{-1}. However, for NO/Pt{111} at coverages below 0.25 ML, Aizawa et al. [9] have shown that although the intensity of the atop band is more intense than that of the hollow site band, intensity transfer does not play a dominant role. Instead, they proposed that a change in electronic structure of the system upon NO adsorption is responsible. On the other hand, the first-principles DFT method has now emerged as a powerful tool to probe the chemistry on transition metal surfaces [5,10–12]. Our previous studies together with those from other groups have shown that the quantities from DFT calculations, such as geometrical structures, adsorption energies and vibrational frequencies, can reproduce experimental values sufficiently well. These DFT results constitute an excellent basis to interpret experimental observations [10–12]. In this work we have applied this technique in combination with RAIRS experiments to resolve the adsorption structures of NO on Ir{100} under various experimental conditions.

2. Experimental and computational methods

2.1. Experimental methods

The Ir{100} single crystal is disc shaped with a diameter of $\sim$8 mm and 1.5 mm thickness. It was cut and mechanically polished to within 0.50° of the crystal plane. Initially the sample was cleaned by repeated cycles of Ar ion sputtering at 900 K, annealing at 1425 K, oxygen treatment at 1160 K and flashing to 1400 K. This procedure produces

a sharp (1×5) low energy electron diffraction (LEED) pattern associated with the quasi-hexagonal reconstruction of the first layer of Ir{1 0 0} atoms, which shows a (1×5) periodicity with respect to the bulk square lattice structure [13–21].

Before recording each set of data the atomically clean (1×5) surface was prepared by Ar ion sputtering at 900 K, followed by annealing at 1400 K, oxygen treatment at 1160 K and finally flashing to 1400 K. Temperature programmed desorption (TPD) has been used on a regular basis to check the cleanliness of the sample. Carbon is the main contaminant in iridium crystals. Therefore, the crystal was considered to be clean when the O_2 TPD spectrum from a given oxygen exposure was reproducible and no CO desorption signal was observed.

The metastable (1×1) phase of Ir{1 0 0} was prepared according to the procedures reported earlier in the literature [16,18,21–23]. According to this procedure 20 L of molecular oxygen is dosed at 475 K, followed by heating the sample to 750 K in order to lift the (1×5) reconstruction completely. The atomic oxygen (oxygen dissociates upon adsorption) is then titrated off by dosing 30 L of CO at room temperature. Finally, the remaining CO is removed by heating the sample to 750 K, which produces a sharp (1×1) LEED pattern. The metastable (1×1) phase is observed up to a temperature as high as 800 K [15,16]. Consistent with this, a theoretical study predicts high activation barrier for self-diffusion of Ir atoms on the surface [23].

The base pressure of the chamber is $\sim 2 \times 10^{-10}$ mbar. All RAIR spectra are recorded continuously through a computer programme at 4 cm^{-1} resolution and are presented as a ratio against a clean surface spectrum. The data acquisition was started after rapidly flashing the sample to 750 K to desorb all gases adsorbed from the background.

2.2. Computational methods

DFT calculations with the generalized gradient approximation (GGA-PBE) [24] were performed using CASTEP [25]. The electronic wave functions are expanded in a plane wave basis set and the ionic cores are described by ultrasoft pseudopotentials [26]. The Ir ultrasoft pseudopotential treats explicitly 5p, 5d and 6s as valence states and non-linear core correction has been included in the pseudopotentials of all the elements. The *relaxation of the semicore 5p state of Ir* was found to be crucial to predict correctly the adsorption site of NO on the Ir{1 0 0} surfaces. The vacuum region between slabs was 10 Å and a cutoff energy of 340 eV was used. Monkhurst–Pack *k*-point sampling with $0.05 \times 2\pi$ $Å^{-1}$ spacing in reciprocal lattice was used for all of the calculations. For example, for a (2×2) unit cell of Ir{1 0 0}-(1×1), $4 \times 4 \times 1$ *k*-point sampling was used. The Ir{1 0 0}-(1×1) and Ir{1 0 0}-(1×5) surfaces have been modelled with five-layers slab with the top two layers relaxed and all the other atoms fixed at the bulk-truncated structure, as shown in Fig. 1. The results of the clean surfaces mimic the LEED I–V structural analysis and DFT results of Johnson et al. [23].

To facilitate the assignment of the infrared spectra observed in experiment, stretching frequencies for adsorbed NO molecules were calculated using a finite-displacement approach [12]. NO stretching frequencies on other surfaces, e.g. Pt{1 1 1}, Pt{2 1 1} and Ir{1 1 1} have been calculated and benchmarked against experiment [12]. It was shown that there is a rigid offset in the calculated NO stretching frequencies, which is attributable to the harmonic approximation and the inherent errors in the DFT-pseudopotential method. This systematic error can be largely avoided by taking the gas phase NO frequency calculation as the reference. In this work, the frequency of the gas phase NO molecule is calculated to be 1916 cm^{-1}, 40 cm^{-1} larger than the experimental value (1876 cm^{-1}). Thus we have subtracted 40 cm^{-1} from each calculated NO frequency, i.e. $\upsilon^{pre} = \upsilon^{cal} - 40$, and the result is given as the predicted value for comparison with experiment. Previous work [10–12,27–30] has demonstrated that the procedure we use for the DFT total energy and vibrational frequency calculations affords good accuracy. In particular, this method of correcting calculated vibrational frequencies is effective [12,29].

3. Results

3.1. NO adsorption on the (1 × 5) phase

Coverage-dependent IR spectra of NO adsorbed at 95 K on the clean Ir{100}-(1 × 5) surface at an ambient pressure of 9×10^{-9} mbar are shown in Fig. 2. Initially two bands grow, at 1815 and 1828 cm^{-1}. With an increase in exposure, the 1828 cm^{-1} band gradually shifts up to 1851 cm^{-1} together with an increase in its intensity while the intensity of the 1815 cm^{-1} band does not change significantly. Also obvious is a third band at 1585 cm^{-1}, which appears at low exposures; its intensity does not change substantially over the exposure range of 1–3 L.

After an exposure of ~2.8 L, equivalent to ~0.3 ML (the calibration procedure is discussed elsewhere [31]), the intensity of the 1851 cm^{-1} band starts to decrease and a band at 1834 cm^{-1} starts to grow in. With further exposure, the 1851 cm^{-1} band completely attenuates and the 1834 cm^{-1} band shifts to 1838 cm^{-1} with hardly any change in the intensity. This occurs over a time span of about 60 s. We observe a decrease in intensity of the fractional order spots of the (1 × 5) surface beyond an exposure of ~2.8 L. This implies the onset of short range lifting of the reconstruction, which is in agreement with the conclusions drawn by Gardner et al. [32].

DFT calculations were then performed to provide further input to the adsorption of NO on the Ir{100}-(1 × 5) phase. NO adsorption on the three most likely high-symmetry sites was investigated, the atop, the bridge and the hollow sites associated with the least coordinated Ir atoms (the outmost Ir atoms) on the surface. The coverage studied is low, 0.1 ML, where the surface remains at the (1 × 5) structure. Previous DFT studies [5,30] have shown that such sites generally have the highest binding ability due to a higher activity of Ir d band. The calculated results are listed in Table 1. The atop site is found to be the most stable, an NO adsorption energy (E_{ad}) of 2.17 eV. This is followed by the bridge (2.09 eV) and the hollow sites (2.04 eV). Importantly, the calculated NO stretching frequencies ($\upsilon_{(NO)}$) at the three sites are well separated, by more than 100 cm^{-1} (Table 1). Based on the calculated adsorption energies and the frequencies, we can readily assign the observed IR bands above 1800 cm^{-1} to the atop NO species, and the 1585 cm^{-1} band to be the bridging NO. The assignment is consistent with the conclusions of Weaver and co-workers [33] who tentatively attributed the NO bands around 1815–1850 cm^{-1} to atop NO species.

Regarding the nature of the two initial atop bands, 1815 cm^{-1} and 1828 cm^{-1}, Gardner et al. [32] have argued that both of them are due to NO at the atop sites of the (1 × 5) surface. Obviously, this is because the Ir{100}-(1 × 5) surface is rather corrugated (Fig. 1b), possessing three distinct types of surface atoms (the previous XPS experiments identified two different surface core level shifts [34,35]). The possibility of these bands being due to other impurities, such as N_2 and CO, can be ruled out as these molecules exhibit different internal stretching frequencies on the Ir{100}-(1 × 5) surface [36,37]. However, in the present work we noticed that at higher exposures the 1815 cm^{-1} band becomes broad but never attenuates completely and only disappears after an exposure of about 2.8 L when the (1 × 5) surface starts to reconstruct to (1 × 1). Thus, the 1815 cm^{-1} band may, alternatively, be interpreted as the stretching frequency of NO at defects, e.g. step edges, since the presence of steps on atomically flat terraces of (1 × 5) surface is supported by the STM experiments [16b,38]. The disappearance of the 1815 cm^{-1} after ~2.8 L of NO exposure would therefore imply that the surface reconstruction initiates from surface defects, which is plausible and is consistent with the previous experimental findings.

3.2. Isotope experiment on the (1 × 5) phase

According to Brown and King [6], NO dimers, $(NO)_2$, on metal surfaces can also exhibit frequencies above 1800 cm^{-1}. In order to further examine the possibility of dimer existence on Ir, we have performed isotopic experiments with a 1:1 mixture of ^{14}NO and ^{15}NO on Ir{100}-(1 × 5). In theory, if each $(NO)_2$ exhibits two 1800 bands due to the symmetric and asymmetric stretches, in the

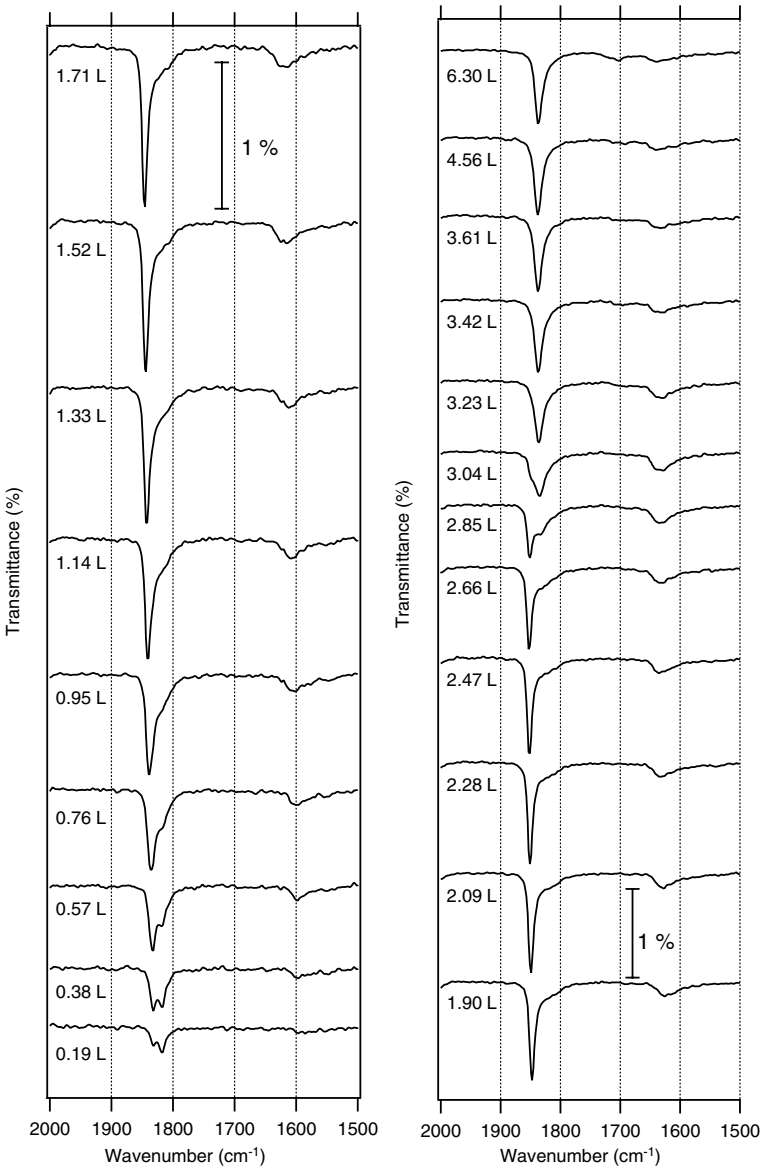

Fig. 2. Coverage and time dependent IR spectra of NO adsorbed at 95 K on the Ir{1 0 0}-(1 × 5) surface at an ambient pressure of 9×10^{-9} mbar pressure. Each spectrum is an integral spectrum within a fixed small time slot (~20 s) using Fourier transform technique. According to the total time and the total number of spectra recorded, the average value of the exposure increment between subsequent spectra is determined to be 0.19 L, as shown in the figure.

presence of a 1:1 mixture of ^{14}NO and ^{15}NO, each of the bands would split into three further bands due to ^{14}NO–^{14}NO, ^{14}NO–^{15}NO and ^{15}NO–^{15}NO couplings [6]. Obviously, the statistical ratio of the integrated IR intensity of these three bands is 1:2:1 in the absence of any dipole coupling [39]. Thus, by checking whether such band splitting happens, the isotope experiment is a good tool to probe the existence of NO dimer.

Fig. 3 shows the coverage-dependent RAIR spectra of a 1:1 mixture of ^{14}NO and ^{15}NO adsorbed on Ir{1 0 0}-(1 × 5) at 95 K. At the low

Table 1
DFT calculated structural parameters, adsorption energy (E_{ad}) and predicted $\upsilon_{(NO)}$ for NO on Ir{100}-(1 × 5)

	Hollow (0.1 ML)	Bridge (0.1 ML)	Atop (0.1 ML)
d(N–O) (Å)	1.228	1.212	1.180
d(N–Ir) (Å)	2.040, 2.073, 2.110	1.956, 1.968	1.770
∠(NO) (°)	85.8	86.4	80.7
E_{ad} (eV)	2.04	2.09	2.17
υ^{pre} (cm^{-1})	1438	1563	1838
υ^{exp} (cm^{-1})		1585	1828

∠(NO) is the angle of adsorbed NO with respect to the ⟨100⟩ surface plane. The deviation of the angle from 90° is due to the corrugation of the (1 × 5) surface. The hollow, bridge and atop sites are labeled in Fig. 1b.

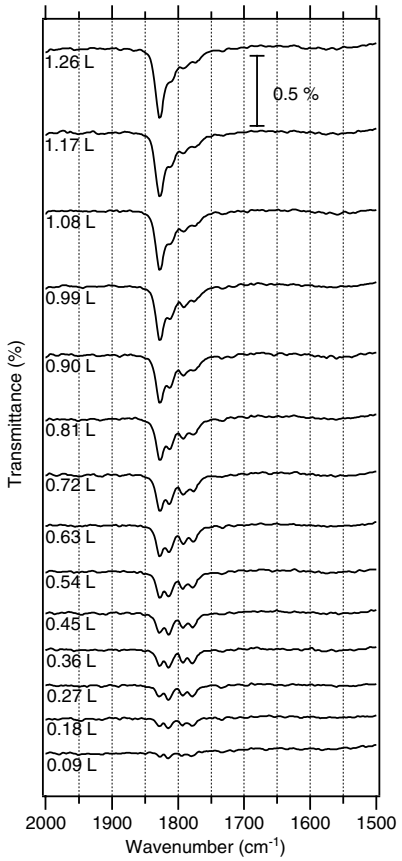

Fig. 3. IR spectra of 1:1 mixture of ^{14}NO and ^{15}NO adsorption on Ir{100}-(1 × 5) at 95 K at an ambient pressure of 2 × 10^{-9} mbar.

exposures four bands are observed, at 1780, 1792, 1815 and 1828 cm^{-1}. These bands replicate those observed in the individual experiments using pure ^{14}NO and pure ^{15}NO. No band splitting occurs. We conclude that at these low exposures no dimer is formed on the surface, and confirm that the two ~1800 cm^{-1} NO bands originate from NO monomers. This is reasonable considering that NO is very strongly bound on Ir (Table 1), which presumably suppresses dimer formation. Low coverage NO dimer formation appears to be restricted to Ag and Cu surfaces [6], where NO monomer bonding with the surface is weak. It is also interesting to notice that the highest frequency band gradually dominates the spectrum with an increase in NO exposure, which demonstrates clearly the intensity transfer caused by dynamical dipole–dipole coupling. Such dipole–dipole coupling does not shift NO frequency much, however, which is apparently due to the intrinsically small dynamic dipole moment of the NO molecule.

3.3. NO adsorption on the (1 × 1) phase

Fig. 4 shows the coverage-dependent RAIR spectra of NO adsorbed at 95 K on the metastable clean Ir{100}-(1 × 1) surface at an ambient pressure of 5 × 10^{-9} mbar. The appearance of NO bands starting from the lowest exposures implies a non-dissociative adsorption for NO on the open (1 × 1) surface. Initially the most pronounced band is at 1585 cm^{-1}. With increase in exposure, this band gradually shifts to higher frequencies. At the same time a second band is observed at 1614 cm^{-1} that shifts to 1653 cm^{-1} at saturation. A third band is observed at 1828 cm^{-1}, which moves to 1817 cm^{-1} at saturation.

DFT calculations for NO adsorption on the (1 × 1) surface are summarized in Table 2. At 0.25 ML (one molecule per (2 × 2) unit cell), the bridge site is found to be the most favored (E_{ad} = 2.41 eV), which is 0.09 eV more stable than that at the atop (E_{ad} = 2.32 eV). The fourfold hollow site NO (E_{ad} = 1.85 eV) is much less stable than the bridging and the atop species. The NO frequencies at these sites are calculated to be 1578 (bridge site), 1845 (top site) and 1411 (hollow site) cm^{-1} (Table 2). Since the hollow site frequency is far smaller than the experimental frequencies and considering its apparent instability,

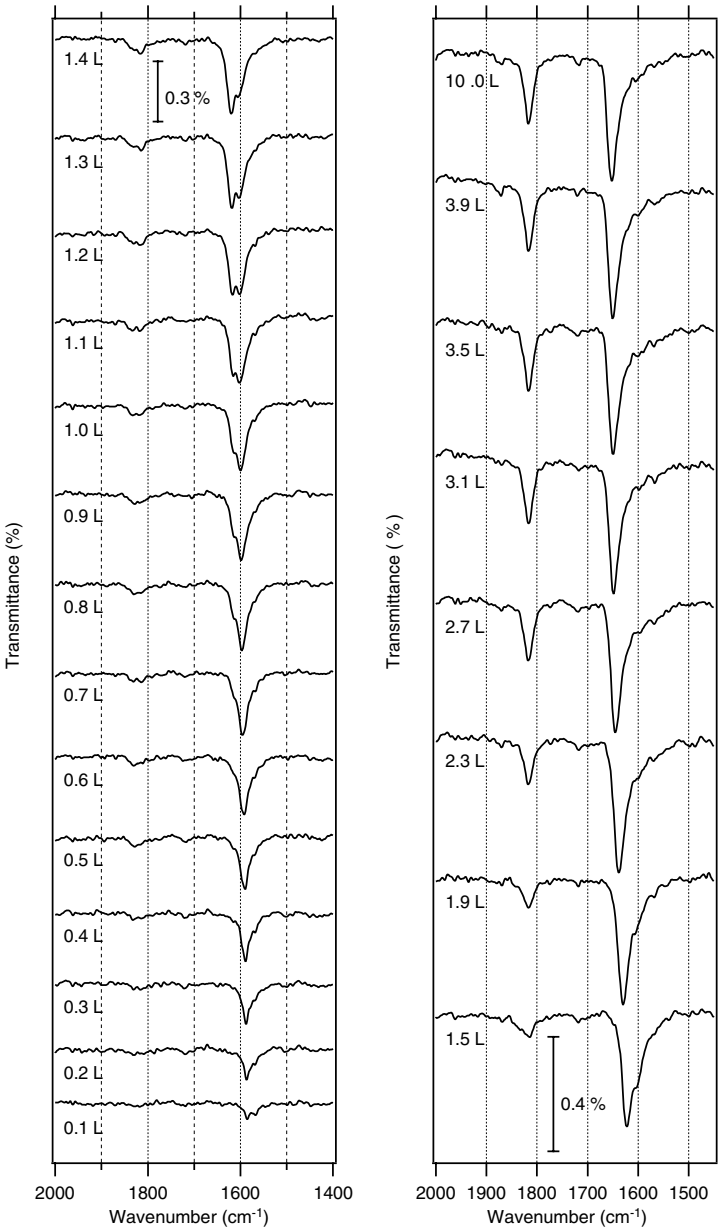

Fig. 4. Coverage-dependent IR spectra for NO adsorbed at 95 K on Ir{1 0 0}-(1 × 1) at an ambient pressure of 5×10^{-9} mbar pressure.

we can assign the 1585–1653 cm^{-1} band to bridging NO, and the 1828 cm^{-1} band to the atop NO. Despite the small adsorption energy difference (0.09 eV) between atop and bridging NO, the DFT result here agrees with the RAIRS observation, which shows that the atop band appears at a later stage in the adsorption sequence (Fig. 4).

By incorporating one more NO in the (2 × 2) unit cell, we further calculated 0.50 ML NO on the (1 × 1) surface (two NO molecules per (2 × 2) unit cell). At this coverage, a c(2 × 2) NO adsorption pattern is found to be the most stable, where NO remains at the bridge site and every surface Ir atom is associated with one NO molecule. The

Table 2
DFT calculated structural parameters, adsorption energy (E_{ad}) and predicted $\upsilon_{(NO)}$ for NO adsorption on Ir{1 0 0}-(1 × 1)

	Bridge (0.25 ML)	Atop (0.25 ML)	Hollow (0.25 ML)	Bridge (0.5 ML)
d(NO) (Å)	1.208	1.180	1.225	1.207
d(N–Ir) (Å)	1.985	1.751	2.301	1.978
E_{ad} (eV/molecule)	2.41	2.32	1.85	2.33
υ^{pre} (cm^{-1})	1578	1845	1411	1574
υ^{exp} (cm^{-1})	1585	1828		

The adsorption sites calculated are labeled in Fig. 1a. In all configurations NO is upright with respect to the ⟨1 0 0⟩ surface plane.

adsorption energy of each NO molecule is 2.33 eV, only 0.08 eV less than that at 0.25 ML. The zone-center (all-in-phase) stretching frequency of NO is calculated to be 1574 cm^{-1}, similar to that at 0.25 ML. The lack of NO–NO coupling at the c(2 × 2) structure may not be too surprising as the NO molecules are quite far apart, with the nearest distance being ~3.8 Å. Considering that the bridge band shifts to 1653 cm^{-1} at high NO exposures in RAIRS, we expect that the saturation NO coverage on Ir{1 0 0}-(1 × 1) is larger than 0.5 ML.

3.4. NO adsorption on the oxygen precovered surface

Ir metal is known to be readily oxidized at temperatures above 600 K and ambient O_2 pressures [40]. The coverage of O atoms on the surface is found to be crucial to the activity of Ir for NO reduction [5]. To study the interplay between the O and NO on the surface, the following experiment was performed. An oxygen-covered Ir{1 0 0} surface was produced by dosing 6.2 L NO on clean Ir{1 0 0}-(1 × 5), followed by flashing the crystal to 800 K to desorb all nitrogen (as N_2), leaving only oxygen adatoms. This produces a p(2 × 1) LEED pattern at room temperature [23]. The structure of the p(2 × 1) O-covered Ir{1 0 0}-(1 × 1) is shown in Fig. 6a, which has been studied in detail using LEED analysis and DFT [23]. Then the crystal was rapidly cooled back to 95 K and NO was again dosed on this oxygen-covered surface.

As shown in Fig. 5, initially two bands develop, at 1649 and 1900 cm^{-1}. With increase in exposure, the 1649 cm^{-1} band gradually shifts to 1672 cm^{-1} whereas the frequency of the 1900 cm^{-1} band does not change significantly. Above an exposure of 2.1 L of NO, the 1672 cm^{-1} band shifts back to 1668 cm^{-1}. At the same time the 1900 cm^{-1} band shifts down to 1894 cm^{-1}, which is accompanied by the surprising appearance of an intense band at 1930 cm^{-1}. With further exposure, the intensities of these bands do not change significantly. It

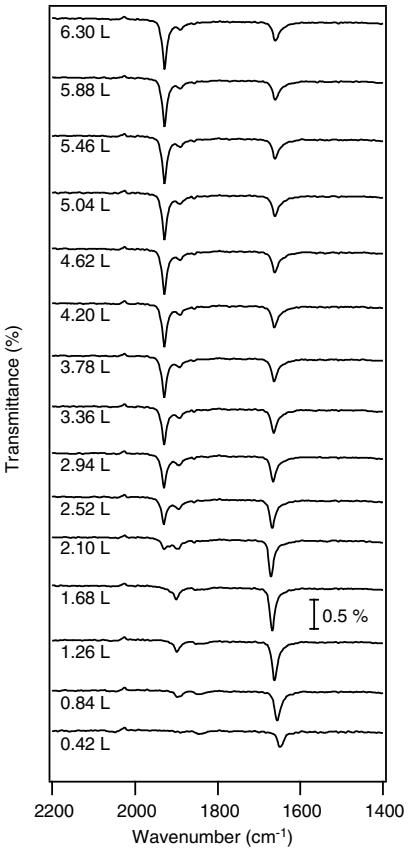

Fig. 5. Coverage-dependent IR spectra of NO adsorption on the oxygen precovered Ir{1 0 0} surface at 95 K.

should be mentioned that unlike the band at 1649–1672 cm^{-1}, the 1900–1930 cm^{-1} bands disappear as the surface is heated up to ~130 K as observed in the independent TP-RAIRS experiment (see Ref. [31]), which indicates that these high-frequency NO species attach only weakly to the surface.

Following the above experiment, NO and O coadsorption was modelled by incorporating NO onto the well-characterized p(2 × 1) O-covered Ir{100}-(1 × 1) [23] (0.5 ML O-coverage). The DFT results are summarized in Table 3. We found that the most stable site for NO on the p(2 × 1) O-covered Ir{100}-(1 × 1) is the remaining empty bridge site (Ir-B, Fig. 6a) on the surface, where each NO can bond with two surface Ir atoms but shares bonding with two neighboring O atoms. In the NO coverage range from 0.125 to 0.25 ML, the NO adsorption energy remains almost constant at ~1.9 eV and decreases to 1.74 eV at 0.50 ML coverage. As a representative, the calculated structure of the 0.25 ML NO and 0.5 ML O coadsorption is shown in Fig. 6b, which exhibits a c(2 × 4) structure. Experimentally, the c(2 × 4) pattern has been observed by LEED and our calculated structure (Fig. 6b) agrees well with the LEED-IV analysis [41]. The stretching frequency of the bridging NO is calculated to be 1642–1687 cm^{-1} at the different coverages (see Table 3), which matches very well with the RAIRS data.

Our calculations also show that NO bonds with the preadsorbed O atoms to form a metastable O–NO complex, with each NO associated with two adsorbed O atoms (site O-B in Fig. 6a). The NO is tilted 62.7° from the surface normal (Fig. 6c and d). The E_{ad}(NO) is calculated to be 0.48 eV and the NO stretching frequency is 1892 cm^{-1}, i.e. higher than the gas phase NO frequency (1876 cm^{-1}). The high frequency of the NO is consistent from the calculated short d(N–O) distance, i.e. 1.153 Å (cf. the gas phase NO distance is calculated to be 1.173 Å). It is likely that this O–NO–O complex is formed by the anti-bonding 2π orbital

Table 3
DFT calculated structural parameters, adsorption energy (E_{ad}) and predicted $\upsilon_{(NO)}$ of NO adsorption on the p(2 × 1) O/Ir{100}-(1 × 1)

NO adsorption site (NO coverage)	Ir-Bridge (0.125 ML)	Ir-Bridge (0.25 ML)	Ir-Bridge (0.50 ML)	O-Bridge (0.25 ML)
d(NO) (Å)	1.197	1.196	1.200	1.153
d(N–Ir) (Å)	1.988	1.984	1.969	
d(N–O_{ad}) (Å)				2.092
E_{ad} (eV/molecule)	1.92	1.91	1.74	0.48
υ^{pre} (cm^{-1})	1642	1648	1687	1892
υ^{exp} (cm^{-1})	1649	1649	1672	1900

The adsorption sites, Ir-Bridge (Ir-B) and O-Bridge (O-B), are labeled in Fig. 6a. The gas phase N–O bond length is calculated to be 1.174 Å. Except for the NO bonding with adsorbed O atoms where the angle is specified in Fig. 6d, NO is upright with respect to the ⟨100⟩ surface plane.

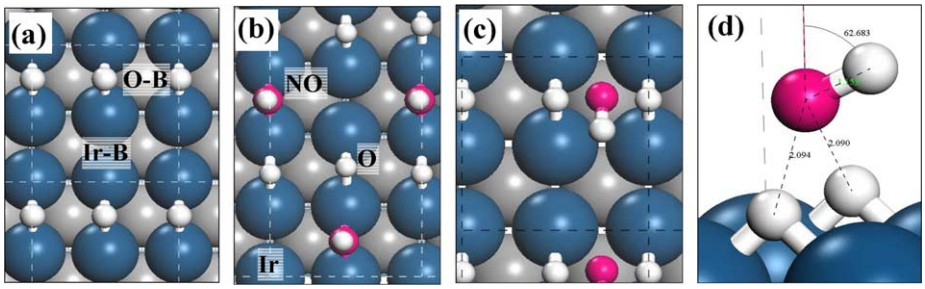

Fig. 6. DFT calculated structures for NO and O coadsorption on Ir{100}: (a) p(2 × 1) structure of O adsorption on Ir{100}-(1 × 1) [23]; (b) c(2 × 4) structure of NO and O coadsorption; (c,d) the top and the side view of NO adsorption on the preadsorbed O atoms.

(lone-pair electron) of NO interacting with the two O adatoms, leading to the loss of electron charge in NO. The so-formed $NO^{\delta+}$ bears a similar high frequency to the NO^{+} ligand in organometallic Ir complexes [42], and a similar O–NO complex has been suggested from a study of NO adsorption on Pt{2 1 1} [12]. Based on these, we conclude that the bands observed at 1900 and 1930 cm^{-1} (Fig. 5) can be assigned to $NO^{\delta+}$ species bonded to a pair of O adatoms.

4. Discussion and conclusions

As mentioned, our RAIRS experiment shows that NO can locally lift the $(1\times5)\rightarrow(1\times1)$ phase reconstruction even at 95 K. This is quite remarkable as the surface reconstruction involves the movement of a large number of surface atoms and is thus expected to occur at high temperatures where the kinetic barrier can be overcome. This is true for the clean surface: the clean metastable (1×1) surface requires a temperature above 800 K to reconstruct to the stable (1×5) phase. To provide insight into the NO induced surface reconstruction, we have examined the thermodynamic possibility of the process by DFT.

From Tables 1 and 2, we know that E_{ad}-(NO) = 2.41 eV on the (1×1) (0.25 ML) and 2.17 eV on the (1×5) surface (0.1 ML). Assuming that E_{ad}(NO) is constant for NO on the (1×1) phase at 0.10–0.25 ML, we find that NO is 0.24 eV more stable on the (1×1) than it is on the (1×5) surface at a coverage of 0.1 ML. On the other hand, the transition of clean (1×1) to clean (1×5) gains 0.16 eV per (2×5) surface area of (1×1) from DFT (equivalent to the surface area of 0.1 ML NO). This comes from the change in the surface energy. Overall, it can be deduced that at the 0.1 ML coverage, NO already enables the (1×1) phase to be energetically more stable (0.24 eV > 0.16 eV) compared to (1×5) phase. Although the energy difference between the two phases appears to be small at 0.1 ML, it should be borne in mind that the energy difference will become more significant as NO coverage is increased. In short, DFT calculations show that the NO-induced (1×5) to (1×1) reconstruction is an exothermic process driven by the strong preference of NO for the more open (1×1) phase. As for the kinetic barrier to the reconstruction, we suspect that the barrier may be largely reduced if the reconstruction initiates from step edges where an open space is available for surface atom migration. These could be the reasons why the process can occur at low temperatures.

As the (1×5) surface starts to reconstruct to the (1×1) at high NO exposures, it is of interest to compare the NO adsorption on the (1×1) and the (1×5) surfaces at high NO exposures. It is expected that the NO adsorption spectra of the two cases should bear some resemblance. From Figs. 2 and 4, we can see that only the atop and the bridging bands are visible in the two cases. However, the details of the two spectra are distinct. First, the NO frequencies are not the same. The atop and the bridge bands on NO/Ir{1 0 0}-(1×5) are at 1838 and 1585 cm^{-1}, respectively; while they appear at 1817 and 1653 cm^{-1} on NO/Ir{1 0 0}-(1×1), respectively. Second, the relative intensity of the two bands is also different. For the (1×1) phase, the atop band is relatively small and the bridge band is intense, while for the (1×5) surface, the atop band is dominant and the bridge band is barely distinguishable. While an atomic-resolution STM image of the reconstructed (1×5) would be desirable to facilitate the explanation of the above difference, here we tentatively provide two possible explanations. (i) The surface reconstruction lifted by NO occurs only locally and the (1×5) surface at high NO exposures is not identical to the (1×1) surface at high NO exposures. (ii) The exact adsorption pattern (local structures, coverages) may well be kinetically controlled, in particular, at the low temperature. As shown, on the Ir{1 0 0}-(1×1) NO prefers the bridge site at the low coverages and it favors the atop site on the Ir{1 0 0}-(1×5). This different site-preference could lead to the different initial NO adsorption pattern in the consequent NO exposures. Our comparative study of NO on Ir{1 0 0} at higher temperatures [31] favors the conclusion that the lifting of the (1×5) structure at 95 K is incomplete and local.

In summary, this work represents a detailed study of NO adsorption on three different

Ir{100} surfaces at 95 K. By combining the RAIRS experiment with DFT calculations, we demonstrate that it is possible to determine the adsorption structure for NO on Ir{100}, where a complex phase transition occurs. The results presented here provide a basis for better understanding the catalytic NO conversion on Ir at high temperatures and high pressures. We have also located an unusual state of adsorbed electropositive NO bridged to a pair of preadsorbed O atoms with an adsorption energy of 0.48 eV.

Acknowledgments

We acknowledge Cambridge Commonwealth Trust (CCT) and EPSRC for financial supports to S.K., the Isaac Newton Trust (Cambridge) for a postdoctoral fellowship (Z-P.L.), the EPSRC for an equipment grant, the UK HPCx and the Cambridge-Cranfield High Performance Computing facility for computer time.

References

[1] M. Nawdali, E. Iojoiu, P. Gelin, H. Praliaud, M. Primet, Appl. Catal. A 220 (2001) 129.
[2] T. Nakatsuji, Appl. Catal. B 25 (2000) 163.
[3] C. Wogerbauer, M. Maciejewski, A. Baiker, J. Catal. 205 (2002) 157.
[4] C. Wogerbauer, M. Maciejewski, A. Baiker, Appl. Catal. B 34 (2001) 11.
[5] Z.-P. Liu, S.J. Jenkin, D.A. King, J. Am. Chem. Soc. 34 (2004) 10746.
[6] W.A. Brown, D.A. King, J. Phys. Chem. 104 (2000) 2578.
[7] A. Crossley, D.A. King, Surf. Sci. 68 (1977) 528.
[8] M.W. Severson, C. Stuhlmann, I. Villegas, M.J. Weaver, J. Chem. Phys. 103 (1995) 9832.
[9] H. Aizawa, Y. Morikawa, S. Tsuneyuki, K. Fukutani, T. Ohno, Surf. Sci. 514 (2002) 394.
[10] P. Hu, D.A. King, M.-H. Lee, M.C. Payne, Chem. Phys. Lett. 246 (1995) 73.
[11] Q.F. Ge, R. Kose, D.A. King, Adv. Catal. 45 (2000) 207.
[12] R.J. Mukerji, A.S. Bolina, W.A. Brown, Z.-P. Liu, P. Hu, J. Phys. Chem. B 108 (2004) 289.
[13] A. Ignatiev, A.V. Jones, T.N. Rhodin, Surf. Sci. 30 (1972) 573.
[14] E. Lang, K. Muller, K. Heinz, M.A. Van Hove, R.J. Koestner, G.A. Somorjai, Surf. Sci. 127 (1983) 347.
[15] N. Bickel, K. Heinz, Surf. Sci. 163 (1985) 435.
[16] (a) K. Heinz, G. Schmidt, L. Hammer, K. Muller, Phys. Rev. B 32 (1985) 6214;
(b) G. Gilarowski, J. Mendez, H. Niehus, Surf. Sci. 448 (2000) 290.
[17] T.N. Rhodin, G. Broden, Surf. Sci. 60 (1976) 466.
[18] J. Kuppers, H. Michel, Appl. Surf. Sci. 3 (1979) 179.
[19] Q. Ge, D.A. King, N. Marzari, M.C. Payne, Surf. Sci. 418 (1998) 529.
[20] M.A. Van Hove, R.J. Koestner, P.C. Stair, J.P. Biberian, L.L. Kesmodel, I. Bartos, G.A. Somorjai, Surf. Sci. 103 (1981) 189, and 218.
[21] G. Kisters, J.G. Chen, S. Lehwald, H. Ibach, Surf. Sci. 245 (1991) 65.
[22] G. Broden, T.N. Rhodin, Chem. Phys. Lett. 40 (1976) 247.
[23] K. Johnson, Q. Ge, S. Titmuss, D.A. King, J. Chem. Phys. 112 (2000) 10460.
[24] J.P. Perdew, K. Burke, M. Ernzerhof, Phys. Rev. B 77 (1996) 3865.
[25] M.C. Payne, M.P. Teter, D.C. Allan, T.A. Arias, J.D. Joannopoulos, Rev. Mod. Phys. 64 (1992) 1045.
[26] D. Vanderbilt, Phys. Rev. B 41 (1990) 7892.
[27] Z.-P. Liu, P. Hu, J. Am. Chem. Soc. 123 (2001) 12596.
[28] Z.-P. Liu, P. Hu, J. Am. Chem. Soc. 124 (2002) 11568.
[29] Z.-P. Liu, P. Hu, J. Am. Chem. Soc. 124 (2002) 5175.
[30] Z.-P. Liu, S.J. Jenkin, D.A. King, J. Am. Chem. Soc. 125 (2003) 14660.
[31] S. Khatua, G. Held, D.A. King, Surf. Sci., submitted for publication.
[32] P. Gardner, R. Martin, R. Nalezinski, C.L.A. Lamont, M.J. Weaver, A.M. Bradshaw, J. Chem. Soc. Faraday Trans. 91 (1995) 3575.
[33] R. Gomez, M.J. Weaver, J. Phys. Chem. B 102 (1998) 3754.
[34] J.F. van der Veen, F.J. Himpsel, D.E. Eastman, Phys. Rev. Lett. 44 (1980) 189.
[35] N.T. Barrett, C. Guillot, B. Villette, G. Treglia, B. Legrand, Surf. Sci. 251 (1991) 717.
[36] P. Gardner, R. Martin, M. Tushaus, J. Shamir, A.M. Bradshaw, Surf. Sci. 287 (1993) 135.
[37] R. Martin, P. Gardner, R. Nalezinski, M. Tushaus, A.M. Bradshaw, J. Electr. Spectrosc. Relat. Phenom. 64 (1993) 619.
[38] L. Hammer, W. Meier, A. Schmidt, K. Heinz, Phys. Rev. B 67 (2003) 125422.
[39] W.A. Brown, P. Gardner, D.A. King, J. Phys. Chem. 99 (1995) 7065.
[40] T. Wang, L.D. Schmidt, J. Catal. 66 (1980) 301.
[41] T.J. Lerotholi, B.C. Russell, S.M. Driver, G. Held, D.A. King, unpublished result.
[42] A. Citra, L. Andrews, J. Phys. Chem. A 104 (2000) 11897.